JOURNAL OF MATERIALS SCIENCE 28 (1993) 4288–4298

Viscoelastic behaviour of composite materials with conventional- or negative-Poisson's-ratio foam as one phase

C. P. CHEN, R. S. LAKES*‡
*Department of Mechanical Engineering, and *Department of Biomedical Engineering and *Center for Laser Science and Engineering, University of Iowa, Iowa City, IA 52242, USA*

This article describes experimental investigations of viscoelastic properties of composites consisting of conventional and re-entrant negative-Poisson's-ratio copper foam as a matrix, with the following high-loss-filler materials: viscoelastic elastomer, solder, and indium. The viscoelastic properties of gallium and several ferrites were also determined. The loss tangent of the copper–elastomer composite substantially exceeded the (lower) Voigt limit; the loss tangent of the copper–solder and copper–indium composites were close to the (upper) Hashin limit for the two-solid phases and one-pore phase.

1. Introduction

An accompanying article considers predictions of the viscoelastic behaviour of composite materials with various structures [1]. Structures which give rise to the highest viscoelastic loss tangent have the common feature that the microscopic distribution of strain is non-uniform so that the deformation kinematics of points in the composite is non-affine. The reason that high loss can arise in composites of this type is that the strain in the lossy, compliant phase is higher than the macroscopic strain in the composite. Non-affine deformation is also characteristic of the recently developed foam materials with negative Poisson's ratios [2, 3]. Experimental studies of conventional and negative-Poisson's-ratio copper foams by holographic interferometry showed that inhomogeneous, non-affine deformation occurred in the ribs of copper foams [4].

The present work is directed at an exploration of model composite materials which exhibit non-affine deformation with the ultimate aim of developing composites with high stiffness and high loss. To that end, the dynamic viscoelastic properties were investigated for composites of both conventional- and negative-Poisson's-ratio copper foams filled with materials of known high loss. This is in contrast to all earlier studies on such foams, which have considered the foam skeleton only, without a second solid phase.

2. Micromechanics-apparatus method

The experimental method made use of a micromechanics apparatus originally developed for the study of Cosserat elasticity in composites, and evolved for the study of viscoelastic materials [5]. The apparatus and associated analysis scheme is capable of determining the viscoelastic properties of a material isothermally, with a single apparatus, over ten decades of time and frequency. Torque was applied to the specimen electromagnetically and its deformation was determined by laser interferometry. Resonances were eliminated from the torque and angle-measuring devices by this approach. Resonances remaining in the specimen itself were corrected by a numerical-analysis scheme based on an analytical solution which is applicable to homogeneous cylindrical specimens of any degree of loss. The apparatus is capable of creep, constant load rate, subresonant dynamic, and resonant dynamic experiments in bending and torsion. The range of equivalent frequency for torsion is from less than 10^{-6} to about 10^{4} Hz.

Analysis of the data to obtain the material's complex shear modulus, $G^* = (\mathrm{Re}(G^*))\ (1 + \mathrm{i}\ \tan\delta)$ is based on a numerical inversion of the following exact relation for the torsional dynamics of a viscoelastic cylinder [6].

$$\frac{M^*}{\Phi} = I_{sp}\,\omega^2\,h\frac{\cot\Omega^*}{\Omega^*} - I_{at}\,\omega^2 \qquad (1)$$

in which M^* is the measured sinusoidal torque applied, Φ is the measured end angular displacement, I_{sp} is the mass moment of inertia of the specimen, ω is the angular frequency in radians per second, $\Omega^* = (\rho\omega^2 h^2/KG^*)^{1/2}$, ρ is the mass density of the specimen, h is the length of the specimen, K is a geometrical constant (1 for a specimen with circular cross-section, 0.8 for a specimen with square cross-section), G^* is the complex shear modulus, and I_{at} is the mass moment of inertia of the end attachment. This analysis scheme incorporates the assumption of a continuous viscoelastic medium. The foams are not

‡ Author to whom correspondence should be addressed.

0022–2461

continuous, but a difference would not become apparent until the resonant frequency of the foam ribs is approached, at frequencies well above those used here. The phase angle between stress and strain was measured with an oscilloscope, as in earlier studies. The resolution of the phase angle on the oscilloscope was approximately 0.7° corresponding to a $\tan\delta$ of 0.012. The loss tangent of low-loss specimens was therefore not obtainable by this method under subresonant conditions at low frequencies. A digital, lock-in amplifier was tried to improve phase resolution, but it generated unacceptable phase errors. A different brand of lock-in amplifier is now being evaluated. The phase resolution was considered adequate for the purposes of this study.

Data reduction in this case of small losses (i.e. $\tan\delta \ll 1$) becomes considerably simplified [6] and errors due to phase uncertainty are reduced [5] in the vicinity of resonance

$$3^{1/2} \tan\delta \approx \frac{\Delta\omega}{\omega_0} \quad (2)$$

The loss tangent, $\tan\delta$, of low-loss materials can therefore be obtained from a specimen of proper size with an external inertia at a resonant frequency via Equation 2. In this study, frequencies associated with vibration and acoustic signals are of particular interest, therefore the lengthy creep experiments used in previous studies are omitted. Experiments were conducted at room temperature (22 °C ± 2 °C); for each individual test, the temperature was constant to within 0.5 °C.

3. Materials

The materials studied included conventional and re-entrant copper foam, solid brass, a high-loss viscoelastic elastomeric polymer, solder (PbSn, 60:40), indium, gallium, and several ferrites. The rationale for the choice of the metals is that, since their melting points are low, viscoelastic losses due to grain-boundary motion or stress-induced diffusion are to be expected at room temperature.

The foams were cut with a low-speed diamond saw (Isomet, Inc.) into prisms of nearly square cross-section. The elastomer was cast in a long rod. The (solid) solder wire was studied in its as-received condition. The indium wire was studied in its as-received condition, following heating at 240 °C and cooling to 20 °C, and following melting at 300 °C and solidification at − 20 °C. The gallium was melted and cast into a plastic tubule. The ferrites were cut with a low-speed diamond saw into slender prisms of nearly square cross-section. The conventional copper foam is open cell with an average cell size of 1 mm, and a density of 680 $Kg\,m^{-3}$ or solid volume fraction 7.6%. The re-entrant copper foam with a cell size of 0.67 mm resulted from a permanent volumetric compression ratio of 1.48. A negative Poisson's ratio as small as − 0.8 can be obtained under these conditions [7]. The specimen sizes were chosen to achieve appropriate structural stiffness for the tests and are shown in Table I.

TABLE I Specimen dimensions

Material	Width (mm)	Length (mm)
Elastomer	6.35 diameter	2.7
Solder	3.125 diameter	228.5
Indium	1.0 diameter	13
Gallium	1.6 diameter	11
Copper	0.85 diameter	65
Brass	1.1 diameter	30
Ferrite, non-magnetic	0.95 square	13.5
Ferrite, magnetic	0.95 square	15
Composite, conventional Cu–elastomer	6.4 square	40
Composite, re-entrant Cu–elastomer	5.4 × 6.9	41
Composite, conventional Cu–solder	5.55 square	38.5
Composite, re-entrant Cu–solder	4.2 × 4.6	31.1
Composite, conventional Cu–indium	4.9 square	36
Composite, re-entrant Cu–indium	4.6	25

Composite specimens were prepared with copper foam as the matrix and polymer, solder, or indium as the fillers. In initial trials, the filler metal was heated by a propane torch or in a furnace, with soldering flux, with the aim of incorporating the melted metal in the voids in the foam. This procedure did not fill the entire void space in the foam with metal, composites prepared in this way had over 50% void volume. Composite foams with low void content were prepared by heating the copper foams and the filler metals in an evacuated glass tube in an oven. This procedure prevented surface oxidation of the copper and improved wetting. The filler metals were melted at approximately 200 °C and deposited into the copper foams by gravity. No oxidation was observed. The void content in the composite foams thus made was found to be less than 15% by volume. Voids with diameters from 0.025 to 0.1 mm were observed microscopically to be scattered inside the foams. No discontinuities between the copper matrix and filler were observed. The injection of viscoelastic elastomer into the copper foams was made courtesy of Polymer Dynamics, Inc., Lehigh Valley, PA, USA.

4. Results and discussion

The dynamic shear modulus $|G^*|$ of solid copper at 1 kHz was found to be 40 GPa and the loss tangent, $\tan\delta$, was 0.002. The loss tangent, $\tan\delta$, of copper at 0.1 Hz is given as about 0.0001 [8].

Graphs of dynamic shear moduli, $|G^*|$, and loss tangent, $\tan\delta$, versus the frequency of foams and solid-filler materials derived from torsional tests are shown in Figs 1–9. The maximum errors in $|G^*|$ and $\tan\delta$ due to the uncertainties in the specimen geometry and measurement accuracies are shown as error bars in Figs 1–9 and Fig. 13. Where no error bar is shown, the estimated error is smaller than the thickness of the data points. Specimen resonances are denoted by downward pointing arrows. Fig. 1 shows results for copper foams of conventional and re-entrant structures. It is observed that the copper foams behave somewhat differently from solid copper since $|G^*|$ and $\tan\delta$ increased substantially at high frequencies.

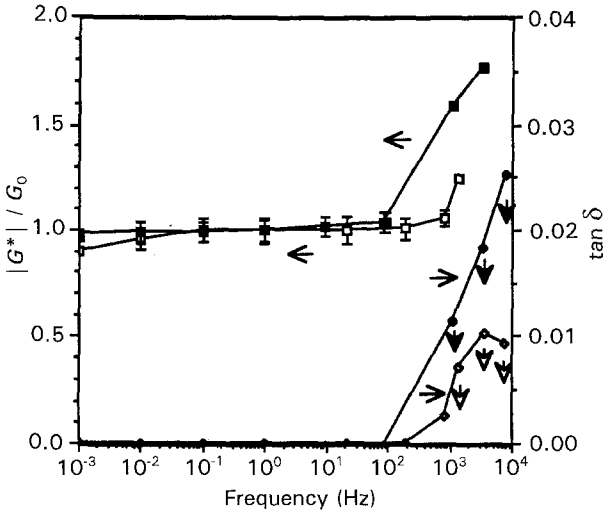

Figure 1 Viscoelastic behaviour of copper foams: (□, ◇) conventional copper foam (volumetric fraction = 7.61%), $G_0 = |G^*(0.1\ \text{Hz})| = 0.0356$ GPa; (■ and ◆) re-entrant copper foam (volumetric fraction = 11.3%), $G_0 = |G^*(0.1\ \text{Hz})| = 0.0268$ GPa.

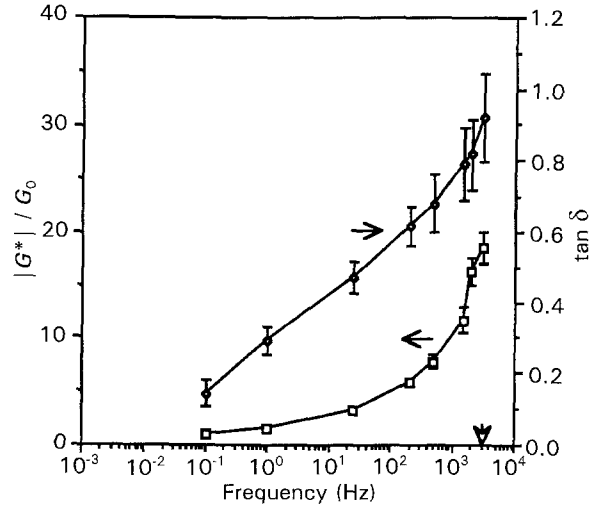

Figure 2 Viscoelastic behaviour of a viscoelastic elastomer polymer. $G_0 = |G^*(0.1\ \text{Hz})| = 0.000131$ GPa.

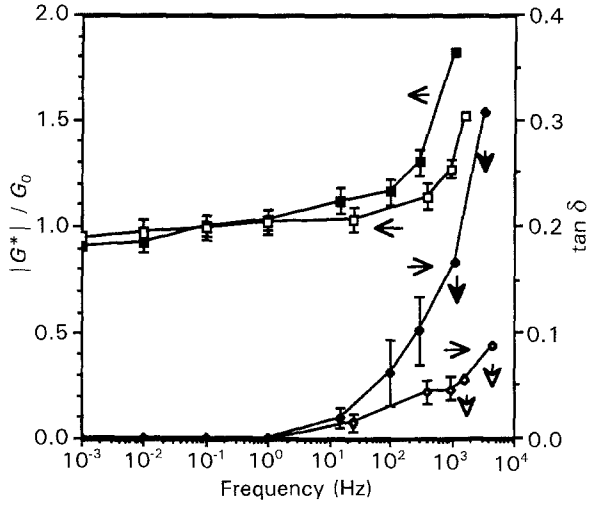

Figure 3 Viscoelastic behaviour of a composite of copper foams and a polymer filler: (□ and ◇) conventional copper foam and polymer (volumetric fraction = 76.1%), $G_0 = |G^*(0.1\ \text{Hz})| = 0.0714$ GPa; (■ and ◆) re-entrant copper foam and polymer (volumetric fraction ≈100%), $G_0 = |G^*(0.1\ \text{Hz})| = 0.0466$ GPa.

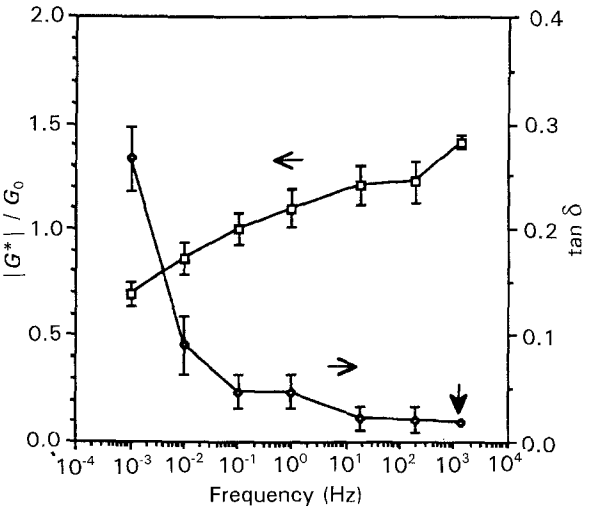

Figure 4 Viscoelastic behaviour of solder. $G_0 = |G^*(0.1\ \text{Hz})| = 9.73$ GPa: (□) $|G^*|/G_0$, (◇) tan δ.

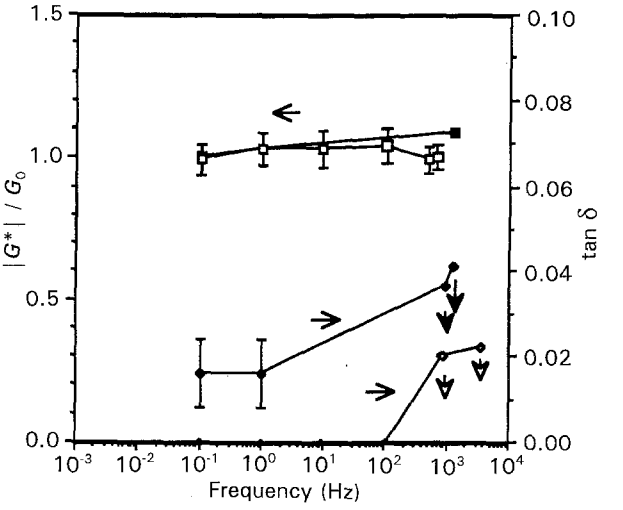

Figure 5 Viscoelastic behaviour of a composite of copper foams and a large void-content-solder-filler: (□ and ◇) conventional copper foam and solder (volumetric fraction = 22.1%), $G_0 = |G^*(0.1\ \text{Hz})| = 0.121$ GPa; (■ and ◆) re-entrant copper foam and solder (volumetric fraction = 33.6%), $G_0 = |G^*(0.1\ \text{Hz})| = 0.263$ GPa.

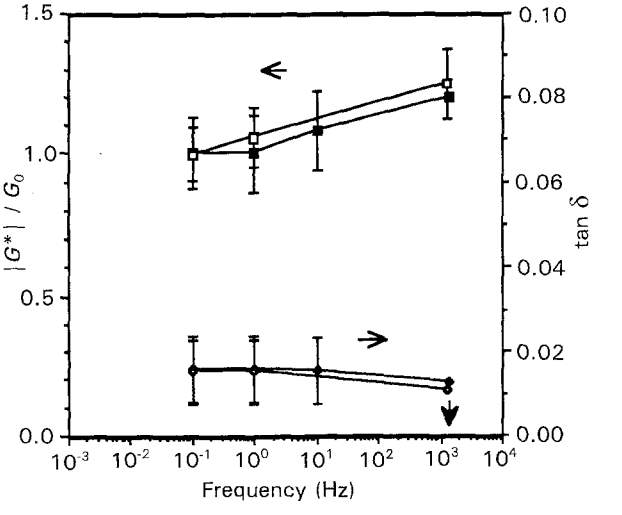

Figure 6 Viscoelastic behaviour of a composite of copper foams and low-void-content-solder filler: (□ and ◇) conventional copper foam and solder (volumetric fraction = 79.9%), $G_0 = |G^*(0.1\ \text{Hz})| = 9.28$ GPa; (■ and ◆) re-entrant copper foam and solder (volumetric fraction = 77.7%), $G_0 = |G^*(0.1\ \text{Hz})| = 11.87$ GPa.

Conventional copper foam exhibits a higher $|G^*|$ than the re-entrant copper foam, which is similar to results observed for the copper and polymeric foams in earlier studies [2]. A higher tan δ is obtained at high frequencies for the re-entrant foam than the conventional foam.

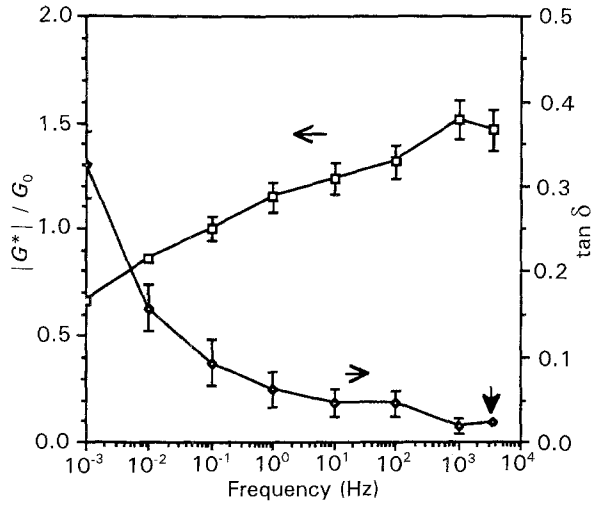

Figure 7 Viscoelastic behaviour of indium. $G_0 = |G^*(0.1\ \text{Hz})| = 2.82$ GPa.

Table II summarizes stiffness and loss results at selected frequencies for the homogeneous materials studied here as well as the copper foams without any filler. The value of the loss tangent for solid copper at low frequency is from Smithells [8]. Table III gives corresponding results for composites based on the foams combined with other materials within the interstices.

Fig. 2 shows results for a viscoelastic elastomeric polymer, which exhibits monotonically increasing modulus and loss tangent. The results of the composites of polymer filler, and conventional and re-entrant copper foams are shown in Fig. 3. The composites show a loss tangent value between those of the solid polymer and foams. However, it is worth noting that the moduli of the composites are almost twice as large than those of the polymer and the foams. This suggests an effect of non-affine deformation.

Fig. 4 shows results for solder. In contrast to the polymeric materials and the copper foams, tan δ for solder decreases when the frequency increases. Fig. 5

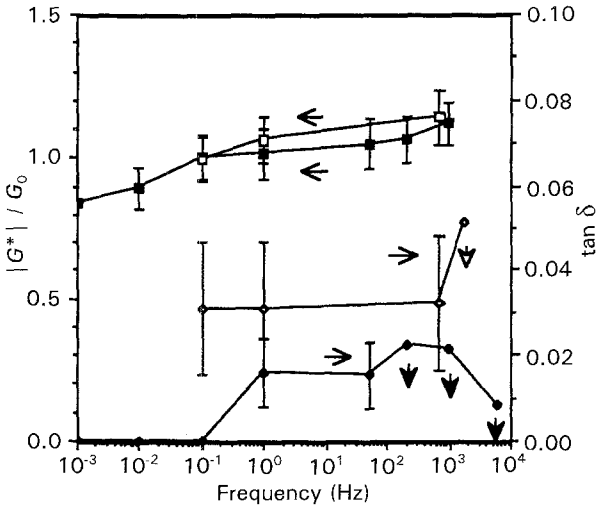

Figure 8 Viscoelastic behaviour of a composite of copper foams and a large-void-content-indium filler: (□, ◇) conventional copper foam and indium (volumetric fraction = 23.4%), $G_0 = |G^*(0.1\ \text{Hz})| = 0.56$ GPa; (■ and ◆) re-entrant copper foam and indium (volumetric fraction = 12%), $G_0 = |G^*(0.1\ \text{Hz})| = 0.103$ GPa.

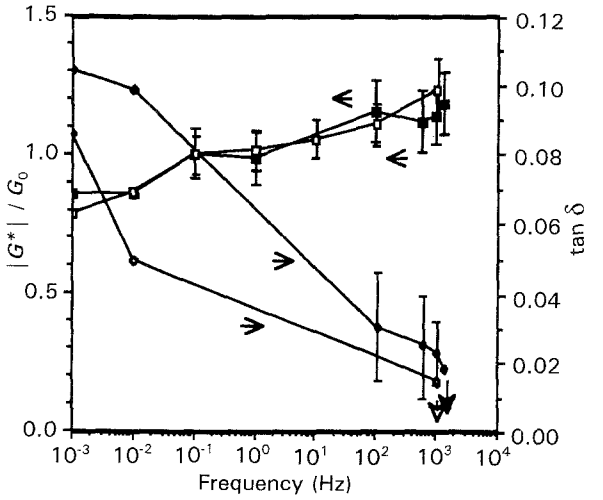

Figure 9 Viscoelastic behaviour of a composite of copper foams and a low-void-content-indium filler: (□, ◇) conventional copper foam and indium (volumetric fraction = 78.5%), $G_0 = |G^*(0.1\ \text{Hz})| = 2.89$ GPa; (■ and ◆) re-entrant copper foam and indium (volumetric fraction = 74.7%), $G_0 = |G^*(0.1\ \text{Hz})| = 4.93$ GPa.

TABLE II Viscoelastic properties of solid materials and foams

Material	Volumetric fraction (%)	0.1 Hz Shear modulus $\lvert G^*\rvert$ (GPa)	Loss tangent tanδ	1 kHz Shear modulus $\lvert G^*\rvert$ (GPa)	Loss tangent tanδ
Solid copper	100	40	≈0.0001	40	≈0.002
Solid brass	100			24	0.0012
Conventional copper foam	7.61(Cu)	0.0356	≤0.012	0.043	0.0068
Re-entrant copper foam	11.3 (Cu)	0.0268	≤0.012	0.0391	0.0134
Polymer (elastomer)	100	1.31×10^{-4}	0.14	1.36×10^{-3}	0.79
Solder	100	9.73	0.0472	13.8	0.018
Indium	100	2.82	0.095	4.27	0.025
Gallium	100	12.6	0.031	16.5	0.033
Magnetic ferrite	100	28.8	≤0.012	32.1	0.055
Non-magnetic ferrite	100	30	≤0.012	30.5	0.021

TABLE III Viscoelastic properties of composite materials

Materials	Volumetric fraction (%)	0.1 Hz Shear modulus $\|G^*\|$ (GPa)	Loss tangent $\tan\delta$	1 KHz Shear modulus $\|G^*\|$ (GPa)	Loss tangent $\tan\delta$
Conventional copper foam + polymer	7.61 (Cu) 76.1 (Polymer)	0.0712	$\leqslant 0.012$	0.0925	0.056
Re-entrant copper foam + polymer	11.3 (Cu) ≈ 100 (Polymer)	0.0466	$\leqslant 0.012$	0.0838	0.167
Conventional copper foam + solder	7.61 (Cu) 22.1 (Solder)	0.121	$\leqslant 0.012$	0.121	0.02
Re-entrant copper foam + solder	11.3 (Cu) 33.6 (Solder)	0.263	0.0157	0.284	0.0366
Conventional copper foam + solder	7.61 (Cu) 79.9 (Solder)	9.28	0.0157	11.0	0.0112
Re-entrant copper foam + solder	11.3 (Cu) 77.7 (Solder)	11.9	0.0157	13.5	0.013
Conventional copper foam + indium	7.61 (Cu) 23.4 (Solder)	0.560	0.0314	0.639	0.0519
Re-entrant copper foam + indium	11.3 (Cu) 12.0 (Solder)	0.103	$\leqslant 0.012$	0.115	0.021
Conventional copper foam + indium	7.61 (Cu) 78.5 (Solder)	2.89	0.0472	3.57	0.0144
Re-entrant copper foam + indium	11.3 (Cu) 74.7 (Solder)	4.93	0.0157	5.58	0.0149

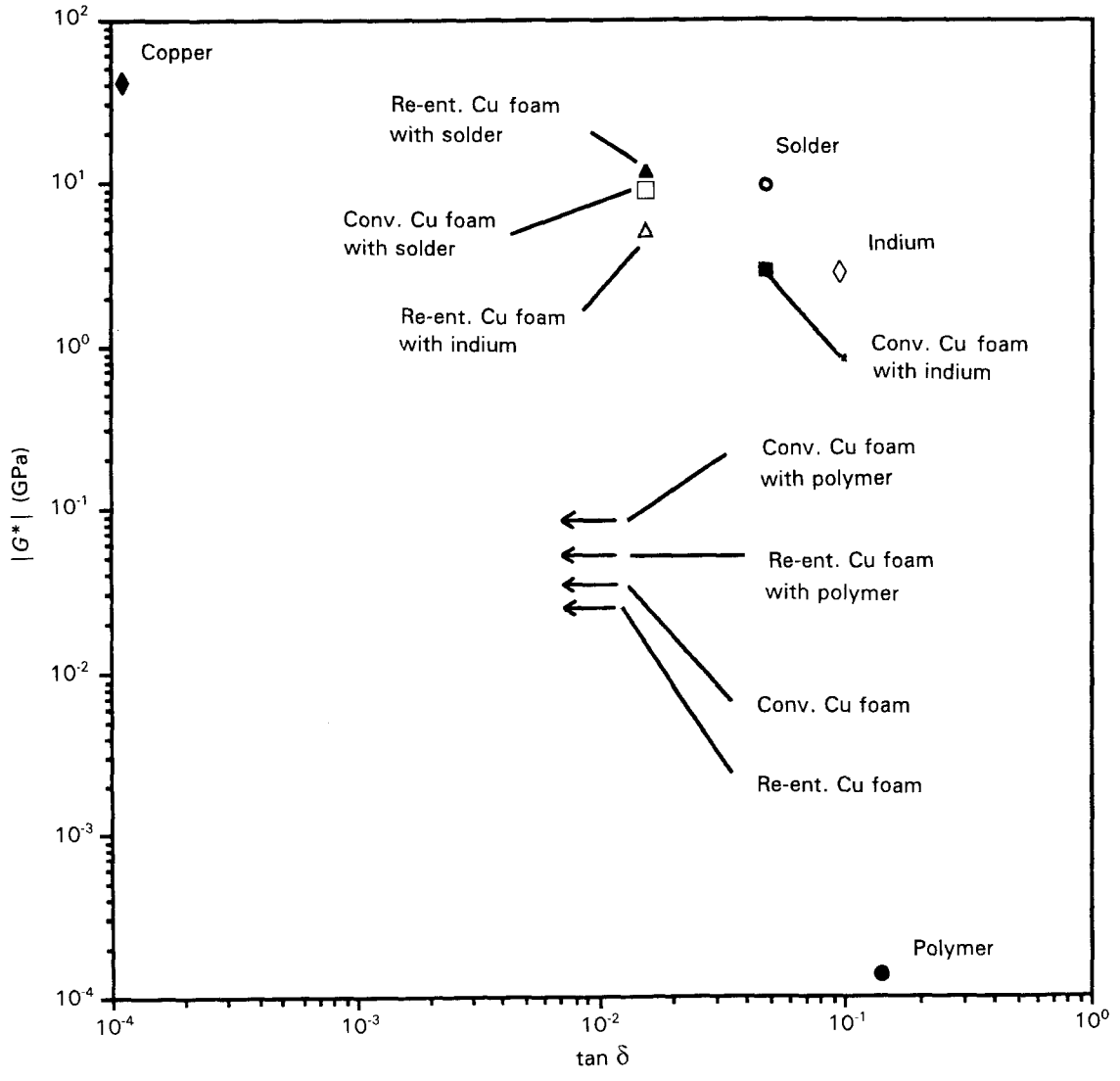

Figure 10 Stiffness–loss map of the viscoelastic behaviour of matrix, fillers, and composites at 0.1 Hz.

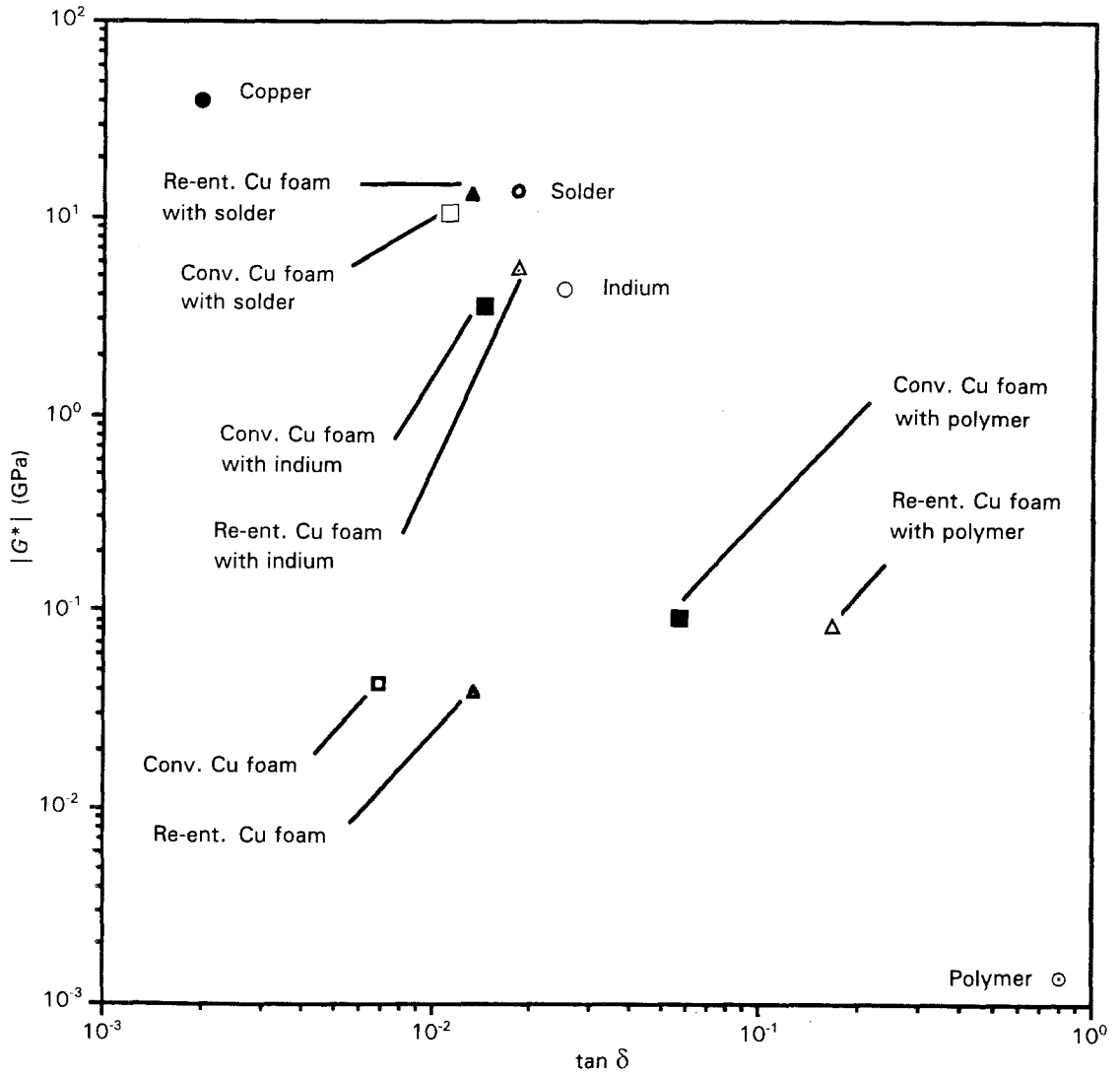

Figure 11 Stiffness–loss map of the viscoelastic behaviour of matrix, fillers, and composites at 1 kHz.

shows results for the conventional, and re-entrant copper foams combined with large-void content-solder filler. The moduli of the composites are only slightly higher than those of the foams; these are much lower than the modulus of the solder, 9.72 GPa at 0.1 Hz. This is as expected since the volumetric fractions of the solder deposited in the foams are low, 22% and 34% for the conventional, and re-entrant foams, respectively. Fig. 6 shows results for the conventional, and re-entrant copper foams combined with low-void-content-solder filler. The moduli at 0.1 Hz of the composites are 9.3 GPa and 11.9 GPa for composites with the conventional and re-entrant foam matrices respectively. The modulus of the composite with the re-entrant copper foam matrix is higher than that with the conventional foam matrix even though the solder fraction in the former is slightly lower than the latter. This is contrast to observations for the pure copper foams and the composites combined with the much softer polymer.

Fig. 7 shows results for indium wire. Fig. 8 shows results for the conventional, and re-entrant copper foams combined with large-void-content-indium filler. Increasing the volume fraction of indium results in a much higher modulus and loss tangent for the conventional copper foam composite in comparison with the re-entrant copper foam composite. Fig. 9 shows results for the conventional, and re-entrant copper foams combined with low-void-content-indium filler. The modulus of the re-entrant copper/indium composite is higher than that of the original copper foam; this behaviour was similar to that of the copper–solder composite.

Figs 10 and 11 show stiffness-loss maps for the copper foams, filler materials and low-void-content composites at 0.1 Hz, and 1 kHz, respectively. For the purpose of comparison, a summary of the constituent volume fractions, and the moduli and loss tangents at selected frequencies is listed in Table III. The moduli of copper foams and polymer composites for the conventional structure were higher than the re-entrant structure. However, the moduli of the solder and indium composites for the conventional structure were higher than the re-entrant structure. The loss tangents, $\tan\delta$, at 1 kHz were always higher for the re-entrant-copper-foam composites than the conventional-copper-foam composites. The large-void-content-indium-filled composites are an exception, in which the volumetric fraction of the indium deposited in the re-entrant copper foam was only half that in the

conventional copper foam. For, the solder-filled and indium-filled composites, large-void-content composites always exhibited higher values of tan δ than low-void-content composites. A possible cause is that the non-affine deformation of the copper skeleton is restrained more when additional metal filler is introduced.

Non-linearities in the composite properties with respect to the strain level were observed. Higher strain levels resulted in lower loss tangents, and a lower

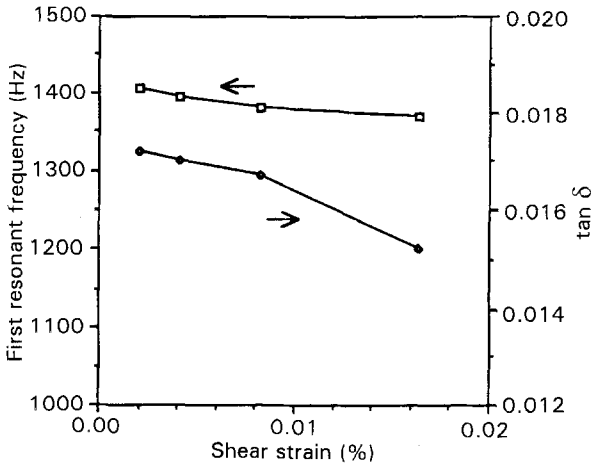

Figure 12 Non-linearity of the first resonant frequency and loss tangent, tan δ, with respect to the strain level. Conventional copper-foam matrix and large-void-content-solder composite, at ≈1 kHz.

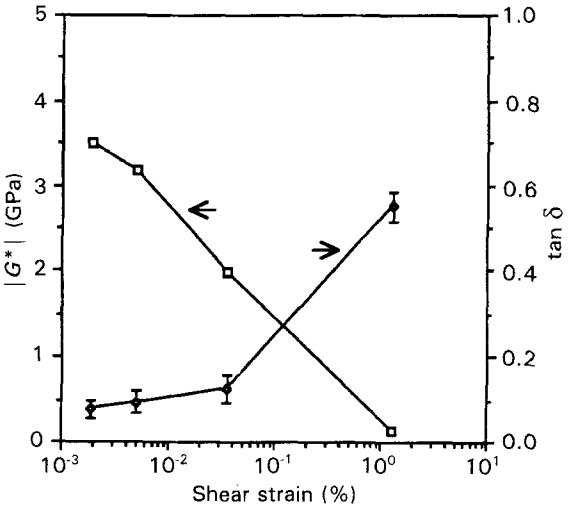

Figure 13 Non-linearity of the shear modulus |G*|, and loss tangent, tan δ, with respect to the strain level for indium at 0.1 Hz.

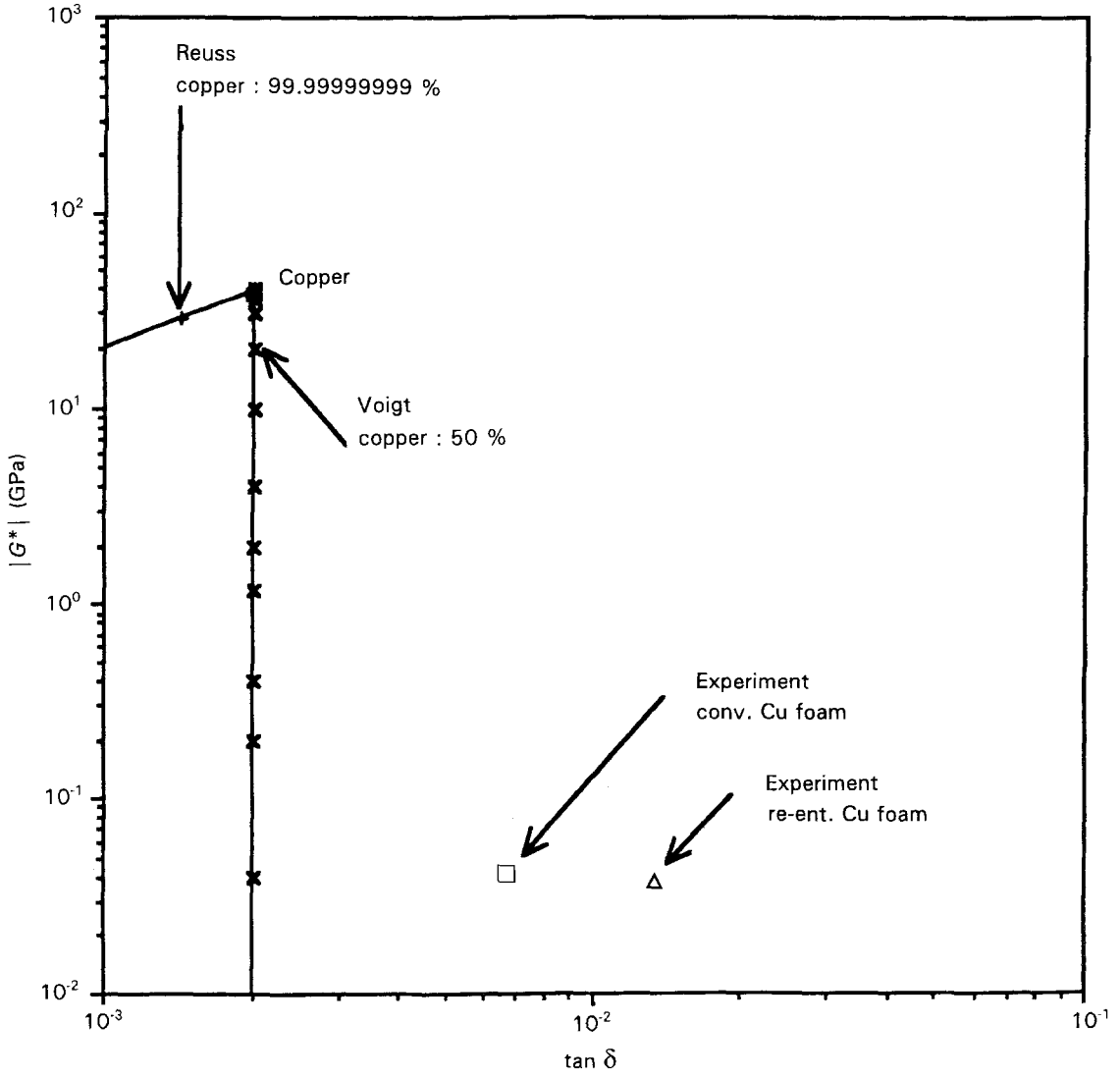

Figure 14 Stiffness–loss map of copper and copper foams: (□) experimental data for conventional copper foam, and (△) experimental data for re-entrant copper foam. Idealized composites of copper foams at 1 kHz: (×) Voigt composite with 50% copper, and (+) Reuss composite with 99.999999998% copper.

modulus for the composite of conventional copper foam and solder, as shown in Fig. 12. A significant increase in the loss tangent at low frequencies was also observed when the strain level was beyond the yield point for indium (which yields at a very low strain), as shown in Fig. 13. For all other experiments, the strain was kept well below the yield point by controlling the input torque.

5. Interpretation of stiffness–loss maps

The viscoelastic properties of composites corresponding to the Voigt, Reuss, and Hashin-Shtrickman bounds on the elastic moduli (for a given volume fraction of one phase) have been determined in a companion article. Such bounds enclose a region on a stiffness–loss map; however it is not yet known if they represent bounds upon viscoelastic properties. Nevertheless, they represent physically realizable composites and they are displayed with the experimental results for the purpose of comparison.

Figs 14–17 show stiffness-loss maps based on measured viscoelastic properties for copper foams and low-void-content-composites at 1 kHz, along with theoretical plots for Voigt, Reuss, and Hashin composites. The Voigt and Reuss curves embody the assumption of only two phases, both solid, hence no voids. The effect of voids in composites with copper, filler, and small pores was incorporated via the multiphase Hashin composite analysis.

The viscoelastic properties of copper foam with no filler are shown in Fig. 14. The loss tangent substantially exceeds that of pure copper at the higher frequencies. This observation is at variance with theory which indicates the loss tangent of a solid is not altered by the presence of voids [9]. That theory agrees with the Voigt curve in Fig. 14. The Reuss curve, however, gives a non-zero stiffness in the presence of voids. This is initially surprising, since in the purely elastic Reuss case one constituent with a stiffness tending to zero results in a composite with stiffness which also tends to zero. However, in the present analysis the void phase was given a small loss which contributes to $|G^*|$. The Voigt and Reuss curves in Fig. 14 were generated by assuming a filler of small stiffness and loss which were then allowed to tend to

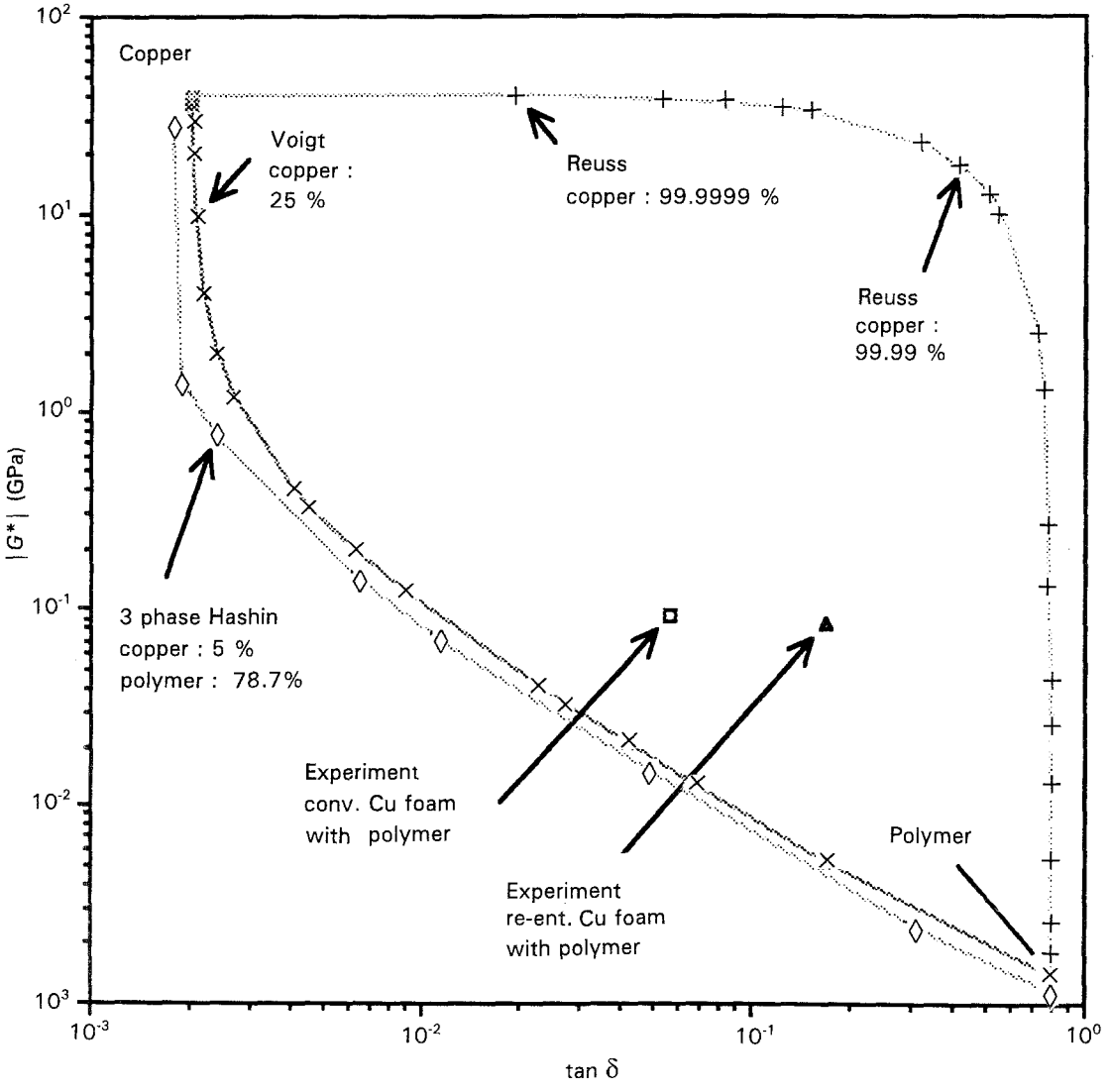

Figure 15 Stiffness–loss map of copper and composites containing copper foam and viscoelastic elastomer polymer. Idealized composites of copper foams and polymer filler at 1 kHz: (×) Voigt composite with 25% copper, (+) Reuss composite with 99.9999% copper, and (◇) the upper bound of a three-phase Hashin composite with 16.3% voids included. (□) experimental data of conventional copper-foam-matrix composite, and (△) experimental data of a re-entrant copper-foam-matrix composite.

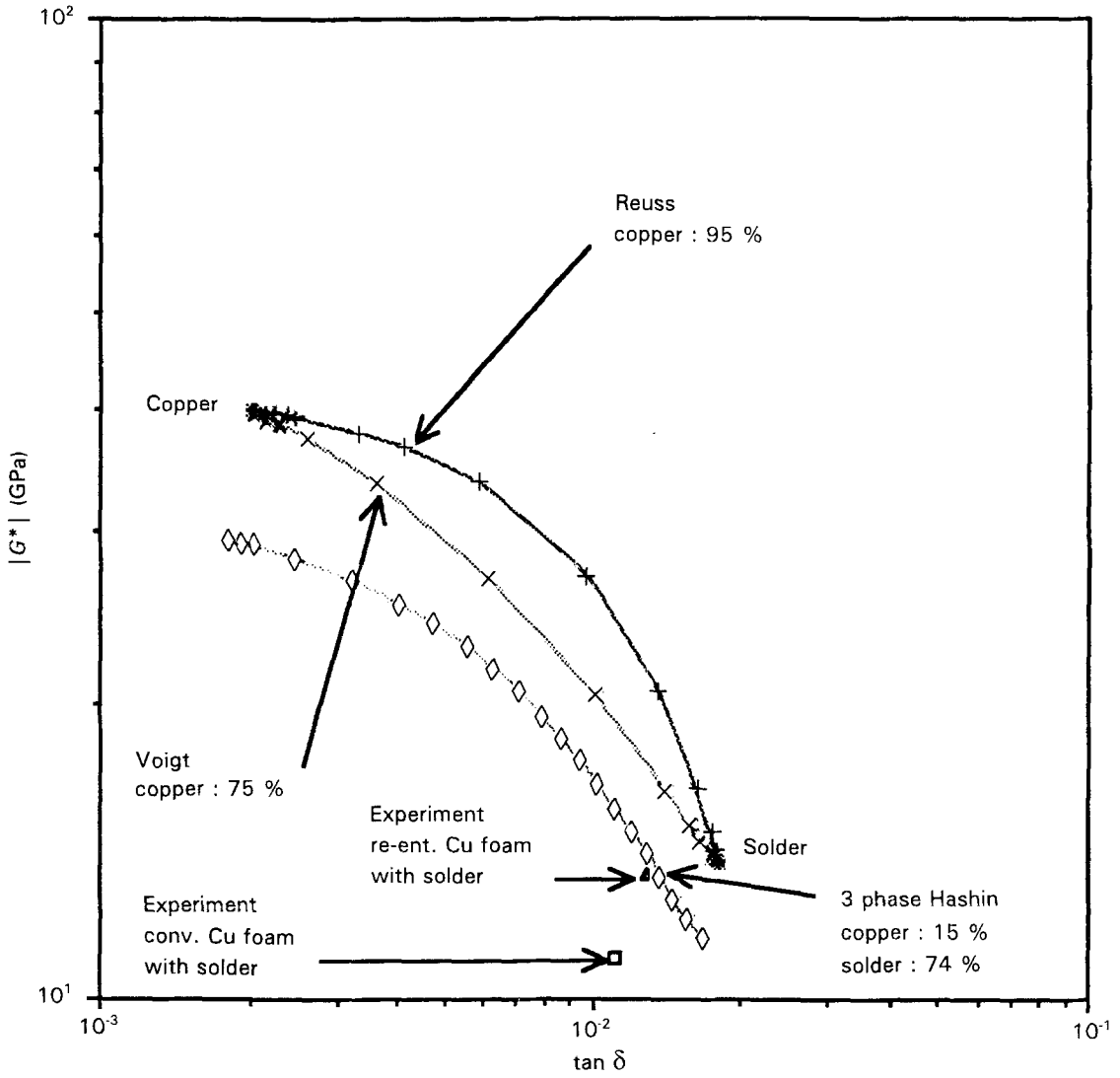

Figure 16 Stiffness–loss map of copper and composites containing copper foam and solder. Idealized composites of copper foams and low-void-content-solder filler at 1 kHz: (×) Voigt composite, (+) Reuss composite, and (◇) the upper bound of a three phase Hashin composite with 11% voids included. (□) experimental data of a conventional copper-foam-matrix composite, and (△) experimental data of a re-entrant copper-foam-matrix composite.

zero. The shape of the curves in the vicinity of the point representing the stiff constituent was insensitive to the ratio of stiffness-to-loss of the void phase during the limiting procedure. The relatively high tan δ experimentally obtained most likely arises from physical processes not included in the elementary analysis. The frequency is too low for the viscosity of air moving in the foam pores to contribute much to the loss, but surface effects in the copper or losses due to cold work may be of interest.

Viscoelastic results of the copper/viscoelastic elastomer composites shown in Fig. 15 lie within the region formed by the Voigt and Reuss curves. Fig. 16 shows the results of the low-void-content-solder-filler foams. For the re-entrant copper foam/solder composite, the experimentally obtained result is close to the data point predicted by the upper Hashin curve; the loss for the conventional-copper-foam composite is somewhat lower. Fig. 17 shows the results of the low-void-content-indium-filler composite. The results are similar to those for the solder-filler composites shown in Fig. 16. The composite with re-entrant copper foam has results closer to the upper Hashin curve than that with conventional-copper composites.

The composites examined in this study all substantially exceeded the (lower) Voigt and Hashin curves in the stiffness–loss map, hence they performed better (in combining stiffness and loss) than would a composite containing spherical compliant inclusions [1]. The composites with two metal phases approached the upper Hashin curve computed allowing for the residual porosity. It is likely that the difference between the metal–polymer composite and the metal–metal composites arises from the degree of restraint on the non-affine unfolding of the copper skeleton, which depends on the stiffness of the filler. None of the composites examined here is as stiff as would be liked in a structural material. The reason is that the volume fraction of the stiff constituent was small in all cases. Nevertheless, they have served as model materials to illustrate the effect of non-affine deformation in composites made with negative-Poisson's-ratio foam. Among the homogeneous materials, a magnetic ferrite displayed a good combination of stiffness and loss,

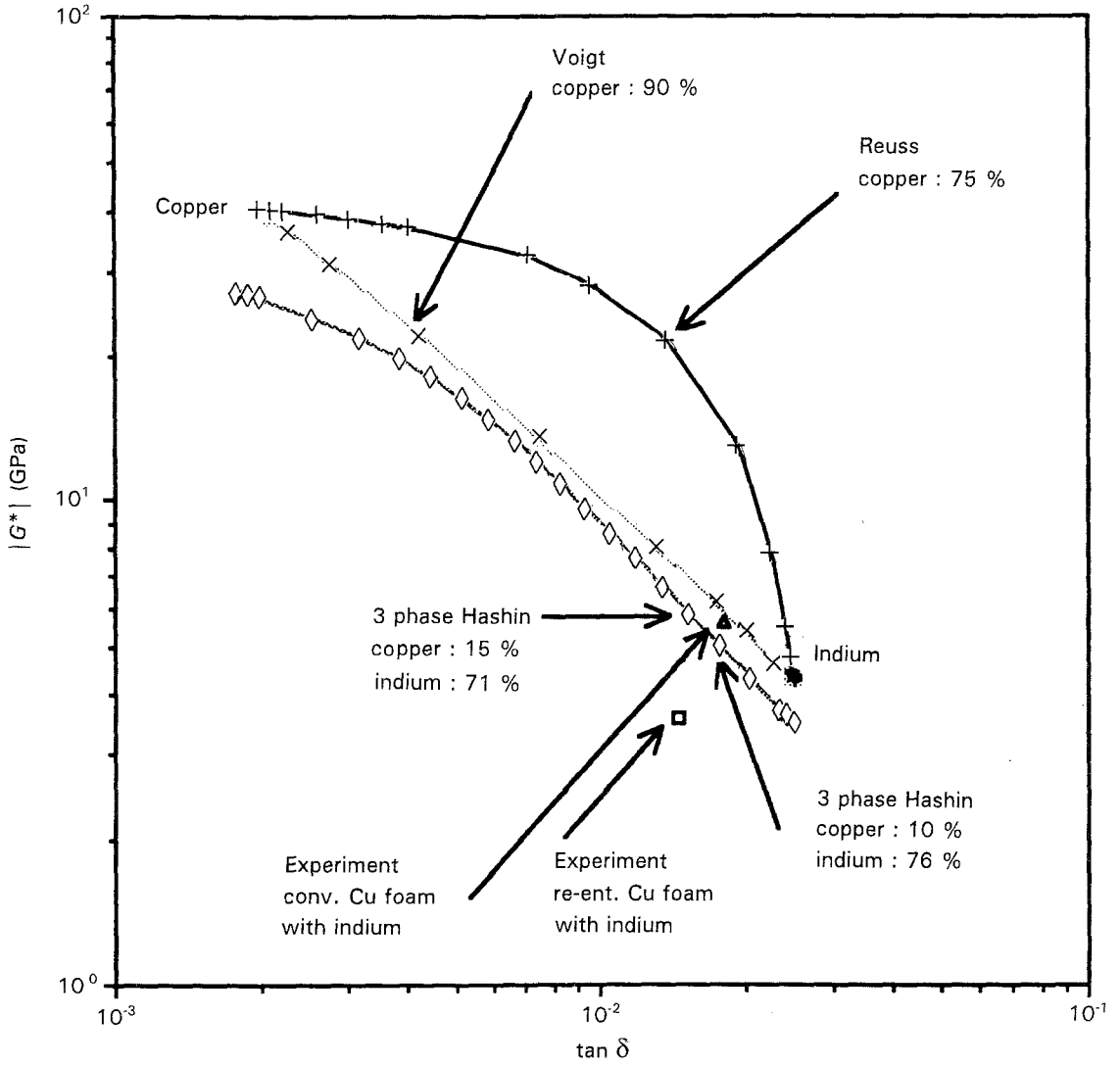

Figure 17 Stiffness–loss map of copper and composites containing copper foam and indium. Idealized composites of copper foams and low-void-content-indium filler at 1 kHz: (×) Voigt composite, (+) Reuss composite, and (◇) the upper bound of a three-phase Hashin composite with 14% voids included. (□) experimental data of a conventional copper-foam-matrix composite, and (△) experimental data of a re-entrant copper-foam-matrix composite.

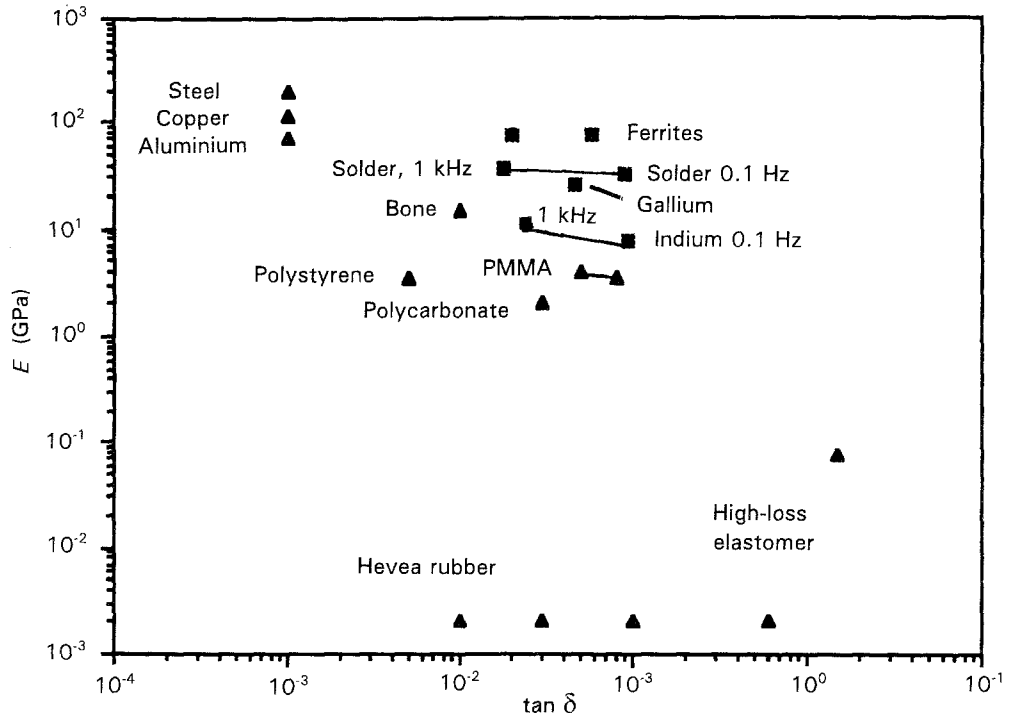

Figure 18 Stiffness-loss map of several materials including solid materials examined in this study: steel, 1 Hz [10], copper, 600 Hz [10], polymethyl methacrylate (PMMA), 10 Hz and 1 kHz [11], bone, 1–100 Hz [12], hevea rubber, 10 Hz to 2 kHz [11], polystyrene, 100 Hz, 1 kHz [11], polycarbonate, 100 Hz [13], viscoelastic elastomer, 100, 1 000 Hz [14].

as shown in Table II and Fig. 18. It may be of interest to incorporate such ferrites in future high-loss composites.

6. Conclusions

1. A viscoelastic elastomer exhibited high loss at high frequency and two high-loss metals, solder and indium, exhibited high loss at low frequencies and comparatively high loss at high frequencies.

2. Viscoelastic properties of copper/viscoelastic elastomer composites exceeded the (lower) Voigt limit. Composites based on re-entrant foams exhibited a higher loss than those based on conventional foam.

3. Composites of copper foam and indium or solder exhibited losses close to the Hashin three-phase upper bound, with the third phase being pore space.

Acknowledgements

We thank the Office of Naval Research for their support of this work. We also thank the University of Iowa for a University Faculty Scholar Award to one of the authors (RSL).

References

1. C. P. CHEN and R. S. LAKES, *J. Mater. Sci.* **28** (1993).
2. R. S. LAKES, *Science* **235** (1987) 1038.
3. R. S. LAKES, *J. Mater. Sci.* **26** (1991) 2287.
4. C. P. CHEN and R. S. LAKES, *J. Mater. Sci.* **26** (1991) 5397.
5. C. P. CHEN and R. S. LAKES, *J. Rheology* **33(8)** (1989) 1231.
6. R. M. CHRISTENSEN, in "Theory of viscoelasticity", 2nd Edn (Academic Press, New York, 1982).
7. J. B. CHOI and R. S. LAKES, *J. Mater. Sci.* **27** (1992) 5373–5381.
8. C. J. SMITHELLS, in "Metals reference book", 5th Edn (Butterworths, London 1976)
9. R. M. CHRISTENSEN, *J. Mech. Phys. Solids* **17** (1969) 23.
10. A. S. NOWICK and B. S. BERRY, in "Anelastic relaxation in crystalline solids" (Academic Press, New York, 1972).
11. J. D. FERRY, in "Viscoelastic properties of polymers", 2nd Edn (John Wiley, New York, 1979).
12. R. S. LAKES, J. L. KATZ and S. S. STERNSTEIN, *J. Biomech.* **12** (1979) 657.
13. I. NIELSEN, in "Mechanical properties of polymers" (Reinhold, New York, 1962).
14. A. T. SHIPKOWITZ, C. P. CHEN and R. S. LAKES, *J. Mater. Sci.* **23** (1988) 3660.

Received 26 August
and accepted 17 November 1992